

The Fabrication and Magnetic Properties of Ni Fibers Synthesized Under External Magnetic Fields

Chunhong Gong,^[a] Laigui Yu,^[a] Yuping Duan,^[b] Juntao Tian,^[a] Zhishen Wu,^[a] and Zhijun Zhang*^[a]

Keywords: Nickel fibers / Nanocrystallites / Chemical reduction / Magnetic fields / Magnetic properties

One-dimensional (1D) nanocrystallites Ni fibers with different lengths were fabricated by the reduction of Ni²⁺ ions by hydrazine hydrate in the presence of external magnetic fields. The effect of the reaction conditions and magnetic field intensity on the microstructures and magnetic properties of the Ni fibers were systematically investigated by scanning electron microscopy (SEM), X-ray diffraction (XRD), and measurement of hysteresis loops at room temperature. It was found that both the intensity of the external magnetic field and the concentration of the nickel salt solution played key roles in governing the microstructures and magnetic properties of the Ni fibers. Namely, the mean length of the Ni fibers increased markedly with increasing Ni²⁺ ion concentration and intensity of the external magnetic field as well. Moreover, the Ni fiber samples prepared under external

magnetic fields had higher squareness and coercivity values than those synthesized in the absence of the external magnetic field. Therefore, a relatively high intensity of the external magnetic field and concentration of the Ni²⁺ ions was selected for the preparation of the desired Ni fibers with improved microstructures and magnetic properties. The present approach has the advantages of having a fast reaction rate and low cost and might be promising for the effective control of the shape and magnetic properties of magnetic materials and for large-scale production as well. The resulting Ni fibers might be potential catalysts, magnetic storage materials, and conductive fillers for shielding of electromagnetic interference (EMI).

(© Wiley-VCH Verlag GmbH & Co. KGaA, 69451 Weinheim, Germany, 2008)

Introduction

One dimensional (1D) magnetic materials have recently been attracting extensive attention because of their fundamental interest and technological applications.^[1–7] Many methods requiring the use of structure-directing templates have successfully been tried for the fabrication of the 1D magnetic materials. To date, a variety of metal nanowire arrays has been produced by electrodeposition with the use of templates.^[8–11] For example, Cao et al. prepared nanotube arrays of Fe, Co, and Ni by electrodeposition on polyaniline membranes.^[8] Ge et al. used the electrodeposition on polycarbonate membranes to prepare Co nanowire arrays with perpendicular anisotropy.^[9] And diblock copolymer^[10] or anodized alumina (AAO) templates^[11] was also used to yield nanowire arrays of excellent quality. As a simple and versatile method, the template-based electrochemical synthesis has been taken as one of the most efficient methods in controlling the growth of nanowires because the

growth can be controlled almost exclusively in the direction normal to the substrate surface. However, template-based synthetic routes have drawbacks in that the introduction of the templates or other additives inevitably adds to the complexity in the synthetic procedures and in the purification of the final products as well. Therefore, it is imperative to develop simple template-free methods for the fabrication of 1D magnetic materials. These materials are more valuable in terms of the expected advantages they present, such as relatively lower cost, higher product purity, and better feasibility for large-scale production.

Previous studies have shown that the magnetic materials can be manipulated by properly adjusting the magnetic field, and field-assisted assembly can be utilized to obtain 1D structures through the induced dipolar effect. For example, Niu et al. and Wang et al. fabricated polycrystalline Co, Ni, and single crystalline Fe₃O₄ wires using the self-assembly of nanocrystallites under external magnetic fields.^[12–14] Zhang et al. prepared chainlike and ringlike Ni–Zn ferrite nanostructures under an external magnetic field, by carefully controlling the thickness of the stabilizing reagent on the surfaces of the ferrite particles.^[15] Athanassiou et al. used a combination of magnetic fields and atmosphere pressure reducing flame to explore the possibility for preparing metallic nanowires at high production rates.^[16] Naturally, 1D nickel nanostructures, as a type of important fer-

[a] Key Laboratory of Special Functional Materials of Ministry of Education, Henan University, Kaifeng 475004, People's Republic of China

[b] School of Materials Engineering, Dalian University of Technology, Dalian 116023, People's Republic of China

Supporting information for this article is available on the WWW under <http://www.eurjic.org> or from the author.

romagnetic materials, have been attracting intensive interest owing to their potential applications in magnetic sensors and memory devices.^[13,17] Because of the shape- and size-dependent properties, one of the main challenges in this area is how to precisely control the shape and crystal structures of the 1D nanostructured Ni products, which is critical to the tailoring of the physical/chemical properties in a controllable way.^[18–20] Unfortunately, previous studies on 1D nickel nanostructures mainly concentrated on the microstructures at a certain external magnetic field in a solvothermal or hydrothermal system, which is less competitive in terms of the facile and simple operation for the fabrication of the magnetic fibers with tunable morphology.

In the present study, therefore, we demonstrate a direct approach for the preparation of Ni fibers under normal pressure in the absence of any inorganic or organic templates, which serves to help easily avoid the introduction of impurities into the final product. The dependence of the morphology of the Ni fibers on the concentration of nickel chloride ($\text{NiCl}_2 \cdot 6\text{H}_2\text{O}$), hydrazine monohydrate ($\text{N}_2\text{H}_4 \cdot \text{H}_2\text{O}$), and sodium hydroxide (NaOH) has been investigated. The effect of the external magnetic field on the morphology of the products was investigated within the magnetic field intensity range 0–0.35 T. Moreover, the magnetic properties of the nanocrystallite Ni fibers were evaluated. The main objectives of the present research are to analyze and optimize the parameters, such as $\text{N}_2\text{H}_4/\text{Ni}^{2+}$ molar ratio, NaOH concentration, Ni^{2+} ion concentration, and intensity of the applied magnetic field, so as to provide clues to factors that control and tune the growth of the Ni fiber nanostructures in engineering.

Results and Discussion

Hydrazine hydrate, as a potent reducing agent in alkali solution, has been successfully used for the syntheses of a variety of nanoscale metal materials because it has a low concentration of impurities and a low cost.^[21] A series of nanocrystallite Ni fibers was prepared from reaction systems containing a fixed concentration of nickel ions (0.01 M) but varied concentrations of $\text{N}_2\text{H}_4 \cdot \text{H}_2\text{O}$ and NaOH in the presence of a 0.3-T external magnetic field at 60 °C, with the aim of revealing the effects of the reducing agent and alkaline on the morphology of the products.

According to Equation (1) (see Experimental Section), the molar ratio of $\text{N}_2\text{H}_4/\text{Ni}^{2+}$ theoretically needs to be kept as 1:2 for the reduction of the dissolved Ni^{2+} ions. However, the reaction system should be kept still and away from any source of agitation to avoid any possible disturbance that may affect the magnetic line of force for the self-assembly of the Ni nanocrystallites. This implies that the diffusion of the reactant ions is confined and a high concentration of the reducing agent is needed to complete the reaction. As evident in our screening experiments, it was impossible to obtain any desired products until the molar ratio for $\text{N}_2\text{H}_4/\text{Ni}^{2+}$ increased to 3. Moreover, once the concentration of $\text{N}_2\text{H}_4 \cdot \text{H}_2\text{O}$ reached a sufficiently high level ($\text{N}_2\text{H}_4/\text{Ni}^{2+} \geq$

3), any further increase in the concentration of $\text{N}_2\text{H}_4 \cdot \text{H}_2\text{O}$ seemed to have little effect on the reduction duration, possibly because of the reduction kinetics.^[22,23] Figure 1(A–D) shows the SEM morphologies of the Ni fibers synthesized from reaction systems with varied molar ratios of $\text{N}_2\text{H}_4/\text{Ni}^{2+}$ and a fixed concentration of NaOH (0.04 M). In general, the Ni fibers prepared from the reaction systems with a molar ratio from 3 to 32 had a few differences both in the SEM morphologies and the reaction times, and therefore a higher molar ratio, for instance 16 and 32, would be beneficial for the formation of uniform and smooth nanocrystallite fibers (Figure 1C and D and Supporting Information Figure S1).

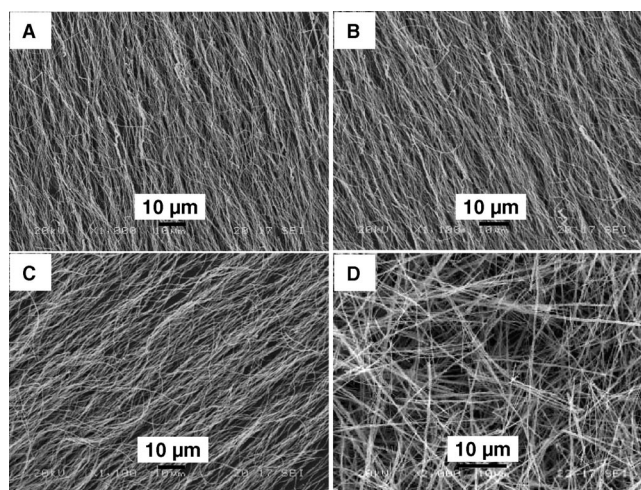


Figure 1. SEM micrographs of the samples obtained at 60 °C from the reaction systems with different $\text{N}_2\text{H}_4/\text{Ni}^{2+}$ molar ratios: (A) 3, (B) 6, (C) 16, and (D) 32.

Similarly, the Ni fibers obtained from the reaction systems with different concentrations of NaOH when the $\text{N}_2\text{H}_4/\text{Ni}^{2+}$ molar ratio was fixed at 32 were also analyzed by means of SEM, in order to shed light on the relationship between the morphology of the target products and the concentration of NaOH in the reaction system under an external magnetic field. To our surprise, an optimal amount of NaOH was imperative for the formation of Ni fibers at a temperature of 60 °C. Namely, no black products were formed in the absence of NaOH until the temperature was increased to 80 °C, which is consistent with that reported in literature.^[22] It was supposed that in the reaction systems containing hydrazine hydrate as a kind of alkali, trace amounts of NaOH do not solely act as a simple alkaline agent but may also act as a catalyst for the formation of Ni nanoparticles. Figure 2 gives the SEM images of the Ni fibers obtained at 60 °C from the reaction systems with different concentrations of NaOH (0.04 M, 0.02 M, and 0.01 M) and the image of the product prepared from the same reaction system at 80 °C but without NaOH for comparison (Figure 2D, reaction duration 60 min). It can be seen that the morphology of the Ni fibers is highly dependent on the concentration of NaOH in the reaction solution. Namely, sample A has almost the same shape as sample B, and these

two samples seem to be more homogeneous and smooth than samples C and D. This could be related to the alkaline-dependent reducing power of hydrazine.^[23] When the concentration of NaOH is sufficiently high ($\text{NaOH}/\text{Ni}^{2+} \geq 2$), some free OH^- ions may remain in the liquid phase and adequate reduction of the nickel ions might be effectively achieved with hydrazine hydrate (Figure 2A and B). The reducing capability of hydrazine hydrate is limited and the reaction rate is reduced at a relatively weaker alkalinity; Ni fibers with a larger roughness and clustered structure were therefore obtained. In contrast, if the molar ratio of NaOH/ Ni^{2+} is too high, the by-product $\text{Ni}(\text{OH})_2$ is generated. Thus, the optimal concentration of NaOH in the reaction system is suggested to be in the range 0.02–0.04 M.

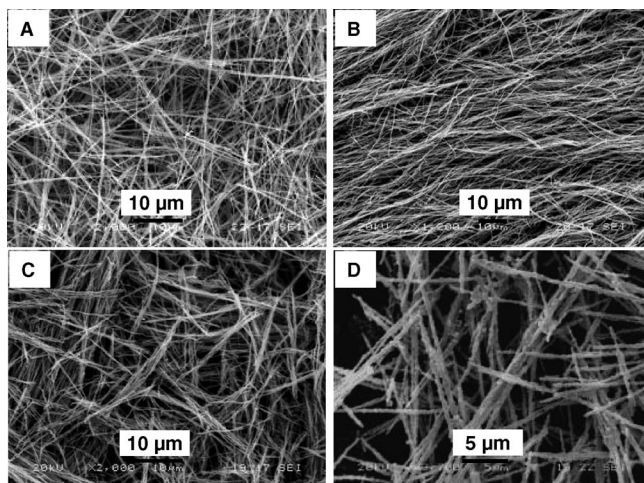


Figure 2. SEM images of nanostructured Ni fibers obtained at 60 °C from the reaction systems with different NaOH concentrations: (A) 0.04 M, (B) 0.02 M, and (C) 0.01 M; (D) shows the image of the product obtained at 80 °C in the absence of NaOH (reaction duration 60 min).

In order to investigate the effect of the concentration of the Ni^{2+} ions on the morphology of the resulting Ni fibers, the reduction was performed in a field of 0.3 T at 60 °C at a fixed $\text{N}_2\text{H}_4/\text{Ni}^{2+}$ molar ratio of 32 and NaOH concentration of 0.040 M but with varied concentrations of the Ni^{2+} ions. It could be worth pointing out that at a Ni^{2+} ion concentration of 0.20 M, a molar ratio of 32 for $\text{N}_2\text{H}_4/\text{Ni}^{2+}$ might be too high in terms of the alkalinity of the N_2H_4 solution and its influence on the volume and component of the solvent. We did a series of preliminary experiments in this respect and found that the nanocrystallite Ni fibers synthesized from the reaction systems containing 0.01 M $\text{NiCl}_2 \cdot 6\text{H}_2\text{O}$ and $\text{N}_2\text{H}_4/\text{Ni}^{2+}$ with varied molar ratios from 3 to 32 had few differences in their morphology, which indicates that the concentration of hydrazine is not a key factor in governing the morphology of the Ni fibers. Bearing in mind our previous finding that Ni^{2+} ions with a concentration of 0.20 M to 0.80 M can be effectively reduced by N_2H_4 at a $\text{N}_2\text{H}_4/\text{Ni}^{2+}$ molar ratio from 6 to 16 in ethylene glycol solvent and under agitation, we chose a molar ratio for $\text{N}_2\text{H}_4/\text{Ni}^{2+}$ of 16 and a Ni^{2+} ion concentration of 0.20 M.

Figure 3 shows the SEM micrographs of the nanocrystallite Ni fibers prepared from the reaction systems containing 0.003–0.20 M of $\text{NiCl}_2 \cdot 6\text{H}_2\text{O}$. It can be seen that the average length of the Ni fibers increase with increasing Ni^{2+} ion concentration, while the average diameter remains about 250 nm. The average length of the Ni fibers prepared at nickel chloride concentrations of 0.003, 0.01, 0.02, and 0.05 M are about 20, 30, 50, and 100 μm , respectively (Figure 3A–D).

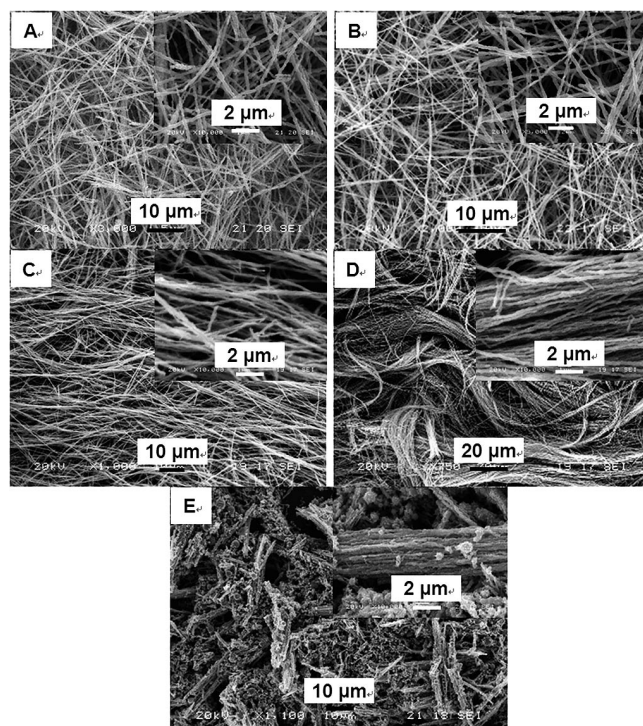


Figure 3. SEM images of the Ni fibers obtained at 60 °C from the reaction systems with different concentrations of Ni^{2+} ions: (A) 0.003 M, (B) 0.010 M, (C) 0.020 M, (D) 0.050 M, and (E) 0.200 M. The insets present higher magnification images.

As a type of classical ferromagnetic materials, Ni crystals have an inherent magnetism and can produce a local magnetic field. When the concentration of the Ni^{2+} ions is increased, the locally induced magnetic field is enhanced too. However, the orientation of each nanocrystallite Ni domain is random unless an external magnetic field is applied. The local magnetic field is induced in the direction of the external magnetic field and strongly enhances the magnetic field when the intensity of the external magnetic field is sufficiently high, which results in a higher magnetic field density. This helps to increase the induced dipole moments and promote the self-assembly process and the orientation of the Ni nanocrystallites. Subsequently, more Ni particles and fibers are assembled together, which results in longer fibers with increasing Ni^{2+} ion concentration. Moreover, when the concentration of the Ni^{2+} ions is sufficiently high (up to 0.05 M), because of the reason already mentioned, the corresponding Ni fibers attract each other in the direction of the magnetic force and experience an enhanced assembling and

aggregating effect, which results in bundlelike self-assembled arrays of Ni fibers with parallel orientation (Figure 3D and E).

When the Ni^{2+} ion concentration in the reaction system reached 0.20 M, a mixture of black product and blue material was obtained at 60 °C even after the reaction period was extended to more than 4 h, which implies that the reducing reaction could not reach completion at this high level of Ni^{2+} ion concentration. The as-synthesized mixture of solid products was characterized by XRD, to evaluate the structure of the blue material. From the XRD pattern (see the Supporting Information Figure S2), in addition to the three characteristic peaks assigned to the Miller indices (111), (200), and (220) of Ni ($2\theta = 44.5^\circ$, 51.8° , and 76.4°), there are indeed some peaks of unknown materials, which cannot be identified as existing nickel compounds such as nickel chloride, nickel chloride hydrate, nickel hydroxide, and nickel oxide et al.. This indicates that the resulting products are composed of fcc Ni and some unknown nickel compound.

The corresponding black product has an irregular microstructure, which is characterized by loosely connected spherulike particulates mixed with a few irregular fibers (Figure 3E). This could be because of the confined diffusion of the Ni^{2+} ions at high concentration levels. Thus, it was suggested to keep the concentration of the Ni^{2+} ions in the reaction system to below 0.05 M so as to ensure the function of the external magnetic field to tailor the morphology and microstructure of the target product.

Nickel fibers could be suitable for electromagnetic shielding as they are good conductors. A small diameter for the metal fibers is preferred because of the skin effect, since the electromagnetic radiation at high frequency interacts only with the near surface region of a conductor. The depth at which the fields are reduced by a factor of $1/e$ is called the skin depth (δ), and it decreases with increasing frequency and conductivity or permeability. The skin depth is dependent on the type of the conductor metal and the frequency of the fields applied to the conductor. As nickel with ferromagnetic nature has a skin depth (δ) of 0.47 μm and 0.33 μm at frequencies of 1 and 2 GHz, respectively,^[24] it can be rationally anticipated that the ultrafine Ni fibers with a diameter size equal to δ or less would be particularly attractive in the fabrication of the composites for electromagnetic interference (EMI) shielding. Up to now, few reports have been available with composites based on nickel fibers or nickel filaments – this might be largely due to the difficulties in the fabrication technique. The fabrication of submicron nickel filaments with a diameter of 0.4 μm by nickel electroplating on carbon filaments with a diameter of 0.1 μm by Chung et al. is one example.^[25] Unfortunately, these nickel filaments had incomplete coverage and poor adhesion to the substrate fibers. Taking into account the significantly increased reaction rate, reduced cost, high yield of Ni fibers, and the feasibility for large-scale preparation of the present approach, we believe it would find promising application in fabricating large quantities of Ni fibers as a type of conductive fillers for EMI shielding, although the

low concentration (not higher than 0.05 M) of Ni^{2+} ions remains a limitation.

Figure 4 shows the XRD patterns of two typical Ni fibers prepared from reaction systems containing 0.05 M and 0.01 M Ni^{2+} ions (the reaction conditions for these two samples are the same as that used for the corresponding samples shown in Figure 3). Three characteristic peaks for Ni ($2\theta = 44.5^\circ$, 51.8° , and 76.4°), corresponding to Miller indices (111), (200), and (220), are observed for both samples, which indicates that they are composed of pure fcc Ni and do not contain impurities (JCPDS 01-1260).^[13] At the same time, the peaks for both samples show obvious signs of broadening, which corresponds to the nanocrystallite structures. The average crystalline sizes of the nanocrystallites were calculated from the half-width of the peaks of (111), by using the Scherrer formula $d = 0.89\lambda/\beta\cos\theta$, to be about 12 nm (Ni^{2+} ion concentration 0.01 M) and 20 nm (Ni^{2+} ion concentration 0.05 M), where λ is the X-ray wavelength, β is the peak width at half-maximum of the corresponding XRD peak, and θ is the Bragg diffraction angle.

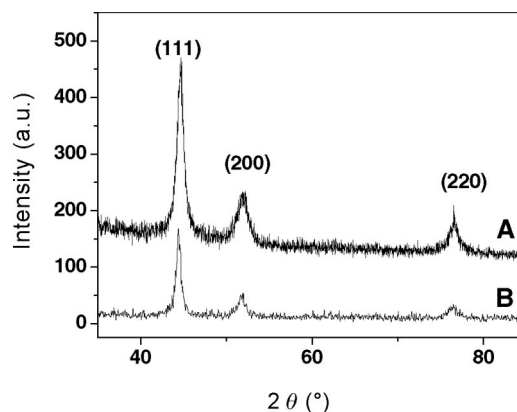


Figure 4. XRD patterns of the Ni fibers obtained at 60 °C from the reaction systems with different concentrations of Ni^{2+} ions: (A) 0.010 M and (B) 0.050 M.

Figure 5 shows the hysteresis loops of the same samples shown in Figure 4. Obviously, the sample derived at a higher Ni^{2+} ion concentration (0.05 M) has an M_s value of

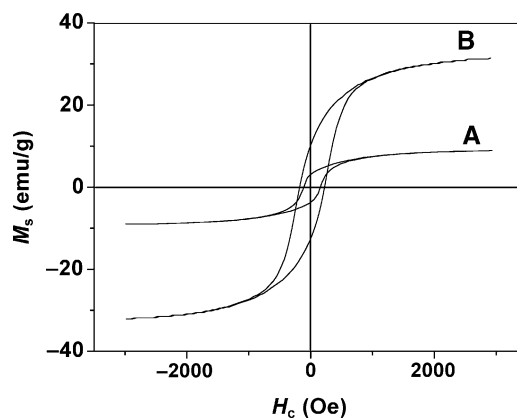


Figure 5. Hysteresis loops of the Ni fibers obtained at 60 °C from the reaction systems with different concentrations of Ni^{2+} ions: (A) 0.010 M and (B) 0.050 M.

31.66 emu/g and an H_c value of 197.57 Oe, which are significantly higher than those of the sample obtained at lower Ni^{2+} ion concentration (8.94 emu/g and 133.8 Oe, respectively). It could thus be concluded that the Ni^{2+} ion concentration has an obvious effect on the morphology and magnetic properties of the nanocrystallite Ni fibers.

A series of samples of nanocrystallite Ni fibers were prepared from the reaction systems with a fixed $\text{N}_2\text{H}_4/\text{Ni}^{2+}$ molar ratio of 32, an NaOH concentration of 0.04 M, a $\text{NiCl}_2 \cdot 6\text{H}_2\text{O}$ concentration of 0.01 M, and at a temperature of 60 °C, but with a varied magnetic field intensity of 0.13, 0.20, 0.22, 0.30, and 0.35, so as to investigate the effect of the intensity of the external magnetic field on the morphology and magnetic properties of the products. Figure 6 shows the corresponding XRD patterns of various Ni fibers samples (coded as sample AF annotated with numeral subscripts, which show the intensity of the magnetic field), as well as the XRD pattern for the product obtained under the same reaction conditions but in the absence of the external magnetic field for comparison (coded as sample ZF). Three characteristic peaks assigned to the Miller indices (111), (200), and (220) of Ni ($2\theta = 44.5^\circ$, 51.8° , and 76.4°) are also observed for this series of samples, which indicates that the resulting products are composed of pure fcc Ni and had no impurities. There are a few differences in the XRD patterns of the ZF and AF samples, and the average crystalline sizes of the samples were calculated, with the Scherrer formula, to be 12, 11, 18, 14, 12, and 9 nm, respectively.

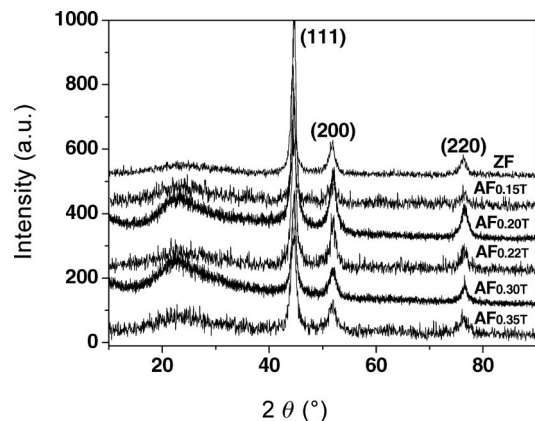


Figure 6. XRD patterns of the ZF, $\text{AF}_{0.13\text{T}}$, $\text{AF}_{0.20\text{T}}$, $\text{AF}_{0.22\text{T}}$, $\text{AF}_{0.30\text{T}}$, and $\text{AF}_{0.35\text{T}}$ samples.

The SEM images of the ZF and AF samples are shown in Figure 7. It is apparent that the morphology of the products depends on the intensity of the external magnetic field. Namely, in the absence of the external magnetic field, short and unsmooth Ni chains are obtained, whose average diameter and length are about 250 nm and 5 μm , respectively. In the presence of the magnetic field with an intensity of not higher than 0.22 T (Figure 7B–D), smooth Ni fibers are obtained, and the average length and diameter of these Ni fibers are marginally different from those of the Ni chains prepared in the absence of the magnetic field. This means that during the chemical reaction, the magnetic field applied has an obvious influence on the nucleation and

growth of the nanocrystallite nickel. In other words, the nanocrystallite Ni could easily nucleate and grow in the direction of the magnetic force rather than randomly in the reaction vessel, which results in fibers and not chains. When the intensity of the magnetic field is increased to 0.3 T (Figure 7E), the corresponding Ni fibers appear to be significantly elongated, and the average length of this type of Ni fiber could be as much as 30 μm . As the intensity of the magnetic field is further increased to 0.35 T, the corresponding Ni fibers are further elongated and characterized by a tangled morphology and a large aspect ratio, and the length of this type of Ni fibers is estimated to be larger than 100 μm (Figure 7F). Therefore, it could be feasible to easily control the length of the Ni fibers by adjusting the intensity of the external magnetic field.

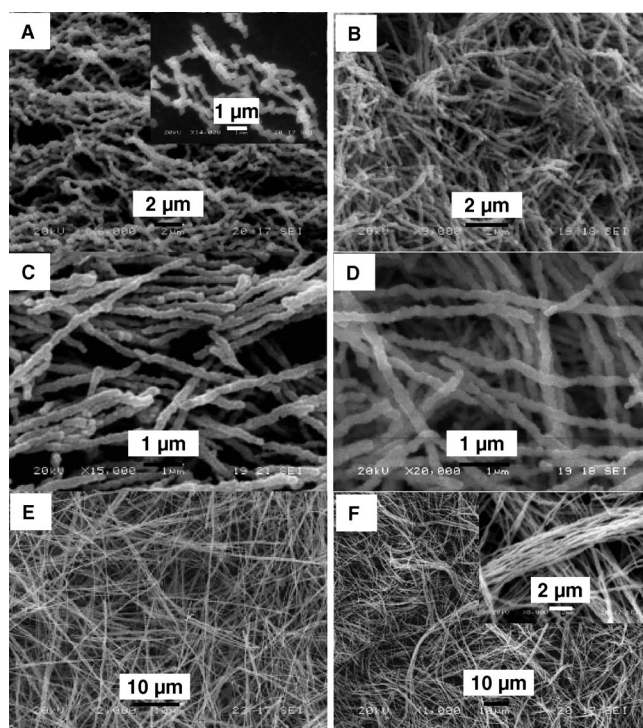


Figure 7. SEM micrographs of samples prepared under different magnetic fields: (A) ZF, (B) $\text{AF}_{0.13\text{T}}$, (C) $\text{AF}_{0.20\text{T}}$, (D) $\text{AF}_{0.22\text{T}}$, (E) $\text{AF}_{0.3\text{T}}$, and (F) $\text{AF}_{0.35\text{T}}$; the insets present higher magnification images.

Because of the complex conditions involved in the growth of the nanocrystallite Ni and the lack of in situ observation facility, it is difficult to describe precisely the growth process of the Ni fibers. It may be primarily inferred, by combining the above-mentioned SEM and XRD results, that whether or not an external magnetic field was applied, the Ni nanocrystallites are first formed during the reduction process, followed by rapid growth in the absence of any additional surfactants that control size and shape. At the same time, the primary Ni crystals could also aggregate together to form spherical particles to decrease the surface energy. When no external magnetic field is applied, the self-assembly process of the Ni crystals may also occur, which results in squiggly Ni chains (see Figure 7A). However, the

self-generated magnetic field of the Ni particles is so weak that the disturbing forces caused by the uneven temperature of the solution and Brownian motion cannot be neglected. Namely, the dipole–dipole interaction having random orientations leads to squiggly Ni chains.

When a magnetic field is applied, as a result of enhanced self-assembly in the direction of the magnetic force under the attraction of the external magnetic field, Ni fibers with a linear structure can be harvested. The fiberlike structures emerge as a result of the combined influence of thermal kinetics and magnetic dipole interactions. Only when endowed with adequate magnetization energy can the particles overcome Brownian motion and align in the direction of the magnetic force, which favors the creation of smooth and straight Ni fibers (otherwise the fibers would be squiggly-shaped), as shown in Figure 7B. If a stronger (e.g. $B = 0.35$ T) external magnetic field is applied, the orientation of the Ni nanoparticles is further promoted, which results in some parallel self-assembled arrays of Ni fibers. Therefore, it is feasible to control the magnetic dipole interactions and hence the length of the Ni fibers by properly adjusting the intensity of the magnetic field applied.

Naturally, the detailed formation process of ferromagnetic fibers is much more complicated than that qualitatively discussed above, because many other factors such as experimental methods, reaction conditions, and reactant types might also affect the aspect ratio of the fibers in the magnetically directed agglomeration process. For example, Sun et al. prepared nickel wires with lengths of up to several hundreds of microns in the presence of magnetic fields, using a solvothermal synthesis route.^[17] They used a mixed solvent of distilled water and ethanol solution and obtained obviously longer Ni wires in the presence of external magnetic fields with a relatively lower intensity (0.10 T and 0.25 T) than in the presence of magnetic fields with a higher intensity (0.40 T), which is just contrary to our finding here (Figure 7). This might be attributed to the use of different types of solvents, which may have a thermodynamic influence on the nucleation velocity and the subsequent growth of the crystals.

Needless to say, it is absolutely necessary to evaluate the magnetic properties of the Ni fibers before they are used as magnetic recording media, sensors, and other devices.^[26,27] Figure 8 shows the magnetic properties of the Ni fibers obtained at different strengths of the external magnetic field. The magnetization vs. magnetic field ($M-H$) loops for the samples were obtained to determine magnetic parameters such as saturation magnetization (M_s), coercivity (H_c), and squareness M_r/M_s (a ratio of the remanent magnetization M_r to saturation magnetization M_s). The ZF sample had an M_s value of 15.07 emu/g, while the AF samples had M_s values of 11.41 (0.20 T), 11.31 (0.22 T), 8.94 (0.30 T), and 30.20 (0.35 T) emu/g. All the samples had smaller M_s values than bulk Ni (55 emu/g),^[28] possibly because of their small sizes as evident by the XRD data (Figure 6). Generally, nanoscale magnetic materials have lower M_s values than the corresponding bulk materials, because the spin disorder on the surface and/or surface oxidation significantly reduces

the total magnetic moment.^[29–31] In addition, the ethylene glycol as a solvent in the reaction system might form a protective layer on the surface of the particles, which reduces the total magnetic moment and hence the M_s values decrease.^[18,32] Interestingly, the sample derived under an external magnetic field of 0.35 T has a large M_s value of 30.2 emu/g, which implies that it could be feasible to meliorate the magnetic properties of desired magnetic materials by applying a strong enough external magnetic field during the synthesis.

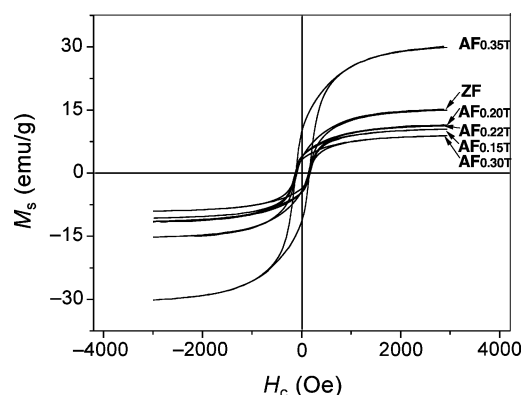


Figure 8. Room-temperature hysteresis loops for the ZF sample and the AF_{0.15T}, AF_{0.20T}, AF_{0.22T}, AF_{0.30T} and AF_{0.35T} samples.

On the other hand, the ZF sample and all the AF samples have a higher coercivity, H_c , than the bulk nickel (100 Oe),^[28] which may be attributed to their special nanostructure, i.e. the reduced size and shape anisotropy of 1D Ni assemblies.^[33,34] In addition, all the AF samples have a significantly increased coercivity (133.8–147.5 Oe) than the ZF sample (115.1 Oe), which is consistent with the observation that all the AF samples have larger values for the squareness (M_r/M_s , 0.36–0.40) than the ZF sample (0.26). The increased H_c and M_r/M_s values of the Ni fibers prepared under an external magnetic field relative to that of the sample in the absence of the external magnetic field may largely be attributed to the oriented growth of Ni nanocrystallites under the attractive force of the external magnetic field,^[6,35,36] which might be well utilized to improve the coercivity of materials as is expected. However, the reasons leading to the differences among the M_r/M_s and H_c values of various AF samples remain unknown at this stage.

It could be interesting to note that the samples obtained at a Ni²⁺ ion concentration of 0.05 M and a magnetic field intensity of 0.30 T have very similar morphologies and magnetic properties to those obtained at a Ni²⁺ ion concentration of 0.01 M and a magnetic field intensity of 0.35 T. Namely, the two groups of Ni fiber samples have a very high aspect ratio of over 500 and a large M_s value, which shows their potential in information storage applications. These fibers have a tendency to aggregate and form bundles, which leads to straight and well self-assembled arrays. In summary, both the intensity of the magnetic field and the Ni²⁺ ion concentration have a drastic influence on the length and magnetic properties of the nanocrystallite Ni fi-

bers. It could be feasible to chemically synthesize novel magnetic materials with improved properties by properly applying an external magnetic field.

Conclusions

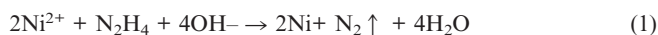
An inexpensive and easy-to-perform route was applied for the fabrication of well-oriented nanocrystallite Ni fibers by chemical reduction at 60 °C in the presence of an external magnetic field. The effect of the magnetic field and reaction parameters such as the nickel salt concentration, reducing agent concentration, and NaOH concentration of the reaction solution on the microstructure and magnetic properties of the Ni fibers were investigated in detail. It was found that the concentration of the nickel salt solution and the intensity of the external magnetic field played key roles in tuning the length and magnetic properties of the Ni fibers. It was found that a relatively high intensity of the magnetic field and concentration of Ni²⁺ ions favor the generation of Ni fibers with increased length and magnetic properties. The present approach, with a fast reaction rate, low cost, high yield, and feasibility for large-scale production may be used for effectively controlling the shape and magnetic properties of magnetic materials and for large-scale production of nanocrystallites. The resulting Ni fibers with different lengths and aspect ratios may have potential applications as catalysts, magnetic storage materials, and conductive fillers for EMI shielding.

Experimental Section

All chemicals of analytical grade were commercially obtained and used without further purification. In a typical process, an appropriate amount of NiCl₂·6H₂O (Tianjin Kermel Chemical Co., Ltd., China) was dissolved in 50 mL of ethylene glycol (EG, Tianjin Kermel Chemical Co., Ltd., China) to form a transparent green solution in a 250 mL beaker, where the concentration of NiCl₂·6H₂O varied from 0.003 M to 0.050 M. An appropriate amount of 80 wt.-% N₂H₄·H₂O (Tianjin Kermel Chemical Co., Ltd., China) solution and 1.0 M NaOH (Tianjin Deen Chemical Co., Ltd., China) solution was then added to the mixed green solution in sequence under strong stirring, which turned indigo within several minutes. To study the effect of an applied external magnetic field on the morphology and magnetic properties of the nickel nanocrystallites, no soluble polymers or other surfactants were used in the present studies.

A NdFeB magnet was placed beneath the beaker used for the reaction to apply an external magnetic field to the reaction system, and the room temperature magnetic field strength on the inner lower surface of the beaker was controlled to be 0.13–0.35 T by adjusting the distance between the beaker and the magnet; the strength of the magnetic field was measured using a Tesla meter. The indigo solution was then allowed to react at a temperature of 60 °C for a few minutes, after which black floccules appeared and the solution turned black. Several minutes later, the solution became clear and colorless, while the desired black fluffy solid product was floating on top of the reaction solution, which indicated the formation of metallic Ni. To ensure that all the reactions reached completion, the time for each reaction process was extended to 0.5–1 h. The

chemical reaction for the synthesis of the nanocrystallite Ni fibers can be expressed as below in Equation (1).



The Ni²⁺ ions were reduced into Ni and were immediately self-assembled into fibers under the magnetic field, and the evolving nitrogen aided in the protection of the nascent nickel nanocrystallites against oxidation.

The as-synthesized solid products were precipitated, separated, washed with ethanol several times, and dried in a vacuum oven at 40 °C for about 24 h. The structures and shapes of the resulting dried samples were characterized by means of X-ray diffraction (XRD, Philips X' Pert Pro X-ray diffractometer; Cu-K α radiation, $\lambda = 0.13418$ nm) and scanning electron microscopy (SEM, JEOL JSM-5600LV; acceleration voltage of 20 kV). The magnetic hysteresis loops of the products at room temperature were measured by using a vibrating sample magnetometer (VSM, Lake Shore 7300).

Supporting Information (see footnote on the first page of this article): SEM micrographs of the samples obtained at 60 °C from the reaction systems with different N₂H₄/Ni²⁺ molar ratios and XRD pattern of the as-synthesized mixture when the Ni²⁺ ion concentration in the reaction system reached 0.20 M.

Acknowledgments

The authors have benefited a lot from the helpful discussion with Prof. Zhen-sheng Jin and Si-xin Wu in our laboratory. The financial support from the Ministry of Science and Technology of China (Grant No. 2007CB607606, in the name of "973" Plan) is acknowledged. Special thanks are due to Dr. Rong Sun at the Center of Precision Engineering, Shenzhen Institute of Advanced Technology, Chinese Academy of Sciences for the VSM characterization.

- [1] N. A. Melosh, A. Boukai, F. Diana, B. Gerardot, A. Badolato, P. M. Petroff, J. R. Heath, *Science* **2003**, *300*, 112–115.
- [2] V. F. Puentes, K. M. Krishnan, A. P. Alivisato, *Science* **2001**, *291*, 2115–2117.
- [3] J. C. Bao, C. Y. Tie, Z. Xu, Q. F. Zhou, D. Shen, Q. Ma, *Adv. Mater.* **2001**, *13*, 1631–1633.
- [4] R. Hertel, *J. Magn. Magn. Mater.* **2002**, *249*, 251–256.
- [5] N. Cordente, M. Respaud, F. Senocq, M. J. Casanova, C. Amiens, B. Chaudret, *Nano Lett.* **2001**, *1*, 565–568.
- [6] M. Z. Wu, Y. Xiong, Y. S. Jia, H. I. Niu, H. P. Qi, J. Ye, Q. W. Chen, *Chem. Phys. Lett.* **2005**, *401*, 374–379.
- [7] M. J. Kim, Y. W. Kim, J. S. Lee, J. B. Yoo, C. Y. Park, *J. Korean Phys. Soc.* **2005**, *47*, 313–317.
- [8] H. Q. Cao, L. D. Wang, Y. Qiu, Q. Z. Wu, G. Z. Wang, L. Zhang, X. W. Liu, *ChemPhysChem* **2006**, *7*, 1500–1504.
- [9] S. H. Ge, C. Li, X. Ma, W. Li, L. Xi, C. X. Li, *J. Appl. Phys.* **2001**, *90*, 509–511.
- [10] T. Thurn-Albrecht, J. Schotter, G. A. Kästle, N. Emley, T. Shi-bauchi, L. Krusin-Elbaum, K. Guarini, C. T. Black, M. T. Tuominen, T. P. Russell, *Science* **2000**, *290*, 2126–2129.
- [11] S. G. Yang, H. Zhu, D. L. Yu, Z. Q. Jin, S. L. Tang, Y. W. Du, *J. Magn. Magn. Mater.* **2000**, *222*, 97–100.
- [12] H. L. Niu, Q. W. Chen, H. F. Zhu, Y. S. Lin, X. Zhang, *J. Mater. Chem.* **2003**, *13*, 1803–1805.
- [13] H. L. Niu, Q. W. Chen, M. Ning, Y. S. Jia, X. J. Wang, *J. Phys. Chem. B* **2004**, *108*, 3996–3999.
- [14] J. Wang, Q. W. Chen, C. Zeng, B. Y. Hou, *Adv. Mater.* **2004**, *16*, 137–140.
- [15] L. X. Zhang, J. Luo, Q. W. Chen, *J. Phys.: Condens. Matter.* **2005**, *17*, 5095–5100.

- [16] E. K. Athanassiou, P. Grossmann, R. N. Grass, W. J. Stark, *Nanotechnology* **2007**, *18*, 165606.
- [17] L. X. Sun, Q. W. Chen, Y. Tang, Y. Xiong, *Chem. Commun.* **2007**, 2844–2846.
- [18] G. Q. Zhang, T. Zhang, X. L. Lu, W. Wang, J. F. Qu, X. G. Li, *J. Phys. Chem. C* **2007**, *111*, 12663–12668.
- [19] J. Wang, Q. W. Chen, B. Y. Hou, Z. M. Peng, *Eur. J. Inorg. Chem.* **2004**, 1165–1168.
- [20] Y. Tang, Q. W. Chen, *Chem. Lett.* **2007**, *36*, 840–841.
- [21] Q. L. Liao, R. Tannenbaum, Z. L. Wang, *J. Phys. Chem. B* **2006**, *110*, 14262–14265.
- [22] S. H. Wu, D. H. Chen, *J. Colloid Interface Sci.* **2003**, *259*, 282–286.
- [23] K. N. Yu, D. J. Kim, H. S. Chung, H. Z. Liang, *Mater. Lett.* **2003**, *57*, 3992–3997.
- [24] X. P. Shui, D. D. L. Chung, *J. Electron. Mater.* **1997**, *26*, 928–934.
- [25] X. P. Shui, D. D. L. Chung, *J. Mater. Sci.* **2000**, *35*, 1773–1785.
- [26] H. Lu, E. L. Salabas, F. Schüth, *Angew. Chem. Int. Ed.* **2007**, *46*, 1222–1244.
- [27] H. Chiriac, T. A. Óvári, A. E. Moga, M. Urse, *J. Optoelectron. Adv. Mater.* **2003**, *5*, 257–260.
- [28] H. Hwang, V. P. Dravid, M. H. Teng, J. J. Host, B. R. Elliott, D. L. Johnson, T. O. Mason, *J. Mater. Res.* **1997**, *12*, 1076–1082.
- [29] J. Wang, Y. J. Zhu, W. P. Li, Q. W. Chen, *Mater. Lett.* **2005**, *59*, 2101–2103.
- [30] V. P. M. S. Kurikka, G. Aharon, P. Ruslan, B. Judit, *Chem. Mater.* **1998**, *10*, 3445–3450.
- [31] P. Fulmer, M. M. Raja, A. Manthiram, *Chem. Mater.* **2001**, *13*, 2160–2168.
- [32] H. B. Xia, J. B. Yi, P. S. Foo, B. H. Liu, *Chem. Mater.* **2007**, *19*, 4087–4091.
- [33] X. M. Liu, S. Y. Fu, *J. Cryst. Growth* **2007**, *306*, 428–432.
- [34] X. M. Ni, Q. B. Zhao, H. G. Zheng, B. B. Li, J. M. Song, D. G. Zhang, X. J. Zhang, *Eur. J. Inorg. Chem.* **2005**, 4788–4793.
- [35] H. H. Lee, H. T. Kuo, K. S. Chou, *J. Chin. Inst. Chem. Eng.* **2003**, *34*, 327–333.
- [36] C. L. Jiang, G. F. Zou, W. Q. Zhang, W. C. Yu, Y. T. Qian, *Mater. Lett.* **2006**, *60*, 2319–2321.

Received: February 24, 2008
Published Online: May 20, 2008